Temperature Dependence of Coherent Oscillations in Josephson Phase Qubits

J. Lisenfeld,[1] A. Lukashenko,[1] M. Ansmann,[2] J. M. Martinis,[2] and A. V. Ustinov[1,*]
[1]*Physikalisches Institut III, Universität Erlangen-Nürnberg, D-91058 Erlangen, Germany*
[2]*Department of Physics and California Nanosystems Institute, University of California, Santa Barbara, California 93106, USA*

(Received 23 April 2007; published 26 October 2007)

We experimentally investigate the temperature dependence of Rabi oscillations and Ramsey fringes in superconducting phase qubits. In a wide range of temperatures, we find that both the decay time and the amplitude of these coherent oscillations remain nearly unaffected by thermal fluctuations. In the two-level limit, coherent qubit response rapidly vanishes as soon as the energy of thermal fluctuations $k_B T$ becomes larger than the energy level spacing $\hbar\omega$ of the qubit. In contrast, a sample of much shorter coherence times displayed semiclassical oscillations very similar to Rabi oscillation, but showing a qualitatively different temperature dependence. Our observations shed new light on the origin of decoherence in superconducting qubits. The experimental data suggest that, without degrading already achieved coherence times, phase qubits can be operated at temperatures much higher than those reported till now.

DOI: 10.1103/PhysRevLett.99.170504 PACS numbers: 03.67.Lx, 74.50.+r, 85.25.Am

Superconducting qubits are electrical circuits based on Josephson tunnel junctions which are fabricated using techniques borrowed from conventional microelectronic circuits. Between various types of rapidly developing superconducting qubits [1–4], the advantages of Josephson phase qubits are their immunity to charge noise in the substrate and simpler fabrication procedures due to relatively large junction sizes. The experimentally controlled degree of freedom in these devices is the superconducting phase difference across a Josephson junction. By now, several groups succeeded in demonstrating coherent oscillations and quantum state manipulation for phase qubits [5–8]. A significant increase of the coherence time in phase qubits became possible after systematic research on microscopic defects in insulator materials [9–11]. These improvements led to the successful demonstration of quantum state tomography tools for phase qubits [12,13].

The decoherence effects in superconducting qubits give rise to a decay of coherent oscillations in the population of the qubit quantum states. One obvious reason for decoherence in Josephson phase qubits is thermal fluctuations, whose effect has not yet been studied. Most experiments so far have been performed at a base temperature of a dilution refrigerator, typically around 15–30 mK, aiming at the lowest achievable temperature in order to obtain the longest possible coherence times. Higher temperatures remain thus unexplored.

We report here systematic measurements of the temperature dependence of Rabi oscillations and Ramsey fringes in Josephson phase qubits. We present experimental data for samples of different origin and made of different materials. In a wide range of temperatures, we find that both the decay time and the amplitude of coherent oscillations, as well as the T_1 time, are rather weakly affected by temperature changes. Samples in the two-state quantum limit show a qualitatively different temperature dependence of the observed coherence times than those operated in the more classical multilevel limit.

A phase qubit uses as its logical quantum states $|0\rangle$ and $|1\rangle$ the lowest two energy eigenstates in a metastable potential well of the Josephson phase in a current-biased junction. An elegant way to decouple the junction from its electromagnetic environment is to apply the bias current through a dc transformer [9] by embedding the junction in a superconducting loop as shown in Fig. 1(a). The resulting circuit is known as rf SQUID and has the potential energy

$$U(\varphi) = \frac{\hbar I_C}{2e}\left[1 - \cos\varphi + \frac{1}{2\beta_L}\left(\varphi - 2\pi\frac{\Phi_{\mathrm{ext}}}{\Phi_0}\right)^2\right], \quad (1)$$

where φ is the phase difference across the junction, I_C is its critical current, Φ_{ext} is the externally applied flux through the qubit loop, and Φ_0 is the superconducting flux quantum. The qubit loop inductance L is chosen such that the parameter $\beta_L = 2\pi L I_C/\Phi_0 \approx 4$, resulting in a double well potential plotted in Fig. 1(b). By adjusting the external magnetic flux close to Φ_0, one of the wells can be made shallow enough to contain only a small number of energy levels. The first excited state $|1\rangle$ in this well can be popu-

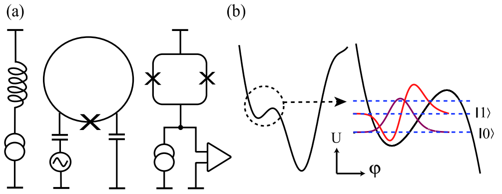

FIG. 1 (color online). (a) Schematic of the phase qubit circuit. The qubit junction is embedded in a superconducting loop which is coupled inductively to the flux-biasing coil and readout dc SQUID. (b) Sketch of the qubit potential $U(\varphi)$. On the right side, a zoom into the shallow left potential well indicates the wave functions describing the two qubit states $|0\rangle$ and $|1\rangle$.

lated by resonant absorption of photons from the applied microwave field. Reading out the state population is done by using an adiabatic dc pulse of magnetic flux, which reduces the height of the barrier separating the wells. The pulse amplitude is adjusted such that a transition from the shallow to the deep well occurs only from excited states. The probability P_{esc} that the readout dc pulse leads to escape from the shallow well, which is our experimental observable, hence directly reflects the population of higher energy states. Since the wells differ by the circulation direction of the loop current, the interwell transition results in a change of magnetic flux, which is registered by recording the switching current of an inductively coupled dc SQUID. After each switching event, a long waiting time of about 1.5 ms assures that no excess heating occurs in the sample chip.

In our measurements, magnetic flux bias was generated by an on-chip coil coupled weakly to the qubit inductance, while microwave currents were supplied through a coplanar transmission line connected capacitively to the qubit junction. The sample temperature was stabilized in the range between 15 and 800 mK. Magnetic shielding was provided by placing the sample in an aluminum-coated copper cell surrounded by a superconducting lead shield and two layers of cryoperm. In order to reduce electromagnetic interference, bias and microwave lines were equipped with cold attenuators, while noise reduction in the dc SQUID wiring was achieved through capacitively shunted copper-powder filters and current dividers at the 1 K temperature stage.

Samples of type no. 1 have been fabricated according to our design at two different foundries [14,15] by using standard lithographic Nb/AlO$_x$/Nb-trilayer processes. A Josephson junction of area 7 μm^2 with a current density of 30 A/cm^2 was embedded into a two-turn loop of inductance $L = 640$ pH to form the qubit. All samples of type no. 1 featured SiO$_2$ as the insulation material between superconducting layers surrounding the junctions.

To directly measure the energy relaxation time T_1, we applied a resonant microwave π-pulse which was separated from the readout dc pulse by a variable delay time. The value of T_1 was extracted from a fit to the resulting exponentially decaying escape probability. All measured type no. 1 samples showed rather small T_1 values below 8 ns. These short lifetimes, in the quantum picture, correspond to broad energy levels.

In order to observe the phase dynamics at higher temperatures, it is essential to avoid thermal activation out of the shallow potential well. The activation rate increases as the potential barrier height becomes comparable to the thermal energy $k_B T$, but is made negligible by reducing the field bias and operating in a deeper potential well. The anharmonicity of the qubit potential has the consequence that the separation between adjacent levels decreases with increasing energy. An external microwave will be resonant with only one transition if the individual levels are not too broad and the potential well is sufficiently anharmonic. Because of their broad energy levels, our Nb-based qubits of type no. 1 can not be regarded as two-state systems when operated in the deep and thus more harmonic potential wells required to avoid thermal activation at higher temperature. The data obtained from these samples thus correspond to multilevel dynamics [6,7], which has been recently shown to have its classical counterpart [16,17].

The temperature dependence of the T_1 time measured on sample no. 1 is plotted in Fig. 2(a). We observe the T_1 time decreasing smoothly from a value of 1.9 ns at 15 mK to 75% of that value at 800 mK. This data has been taken in a deep potential well; the frequency of a resonant microwave π-pulse was 16.5 GHz. For the same sample and parameters, Fig. 2(b) shows oscillations of the escape probability observed by varying the duration of an applied resonant microwave pulse followed by the dc-readout pulse. The oscillations were fitted by an exponentially damped sine to extract their frequency, amplitude and decay time. While the oscillation frequency depends linearly on the applied microwave amplitude for small amplitudes, as it is expected for Rabi oscillation, it bends off to lower frequencies at higher drive amplitudes. At a temperature of 15 mK, the oscillations had 70% to 80% visibility and decayed at a rate of typically 3 to 5 ns. Both oscillation amplitude and decay time were found to vary smoothly with temperature. At 0.8 K, the amplitude was reduced by a factor of 1 half, while the oscillation decay time dropped only to 80%. Because of the short coherence times of sample no. 1, we could not directly measure the dephasing time T_2^* by a Ramsey-type experiment.

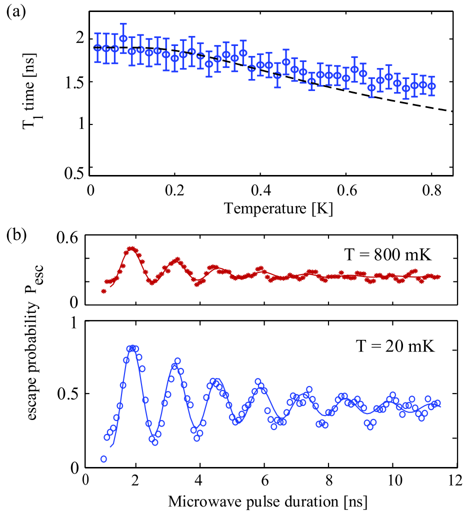

FIG. 2 (color online). (a) Temperature dependence of the T_1 time of Nb-based sample no. 1, measured by monitoring the lifetime of the excited state after populating it by a resonant π-pulse of duration 1.9 ns and frequency 16.5 GHz. The dashed line is a plot of Eq. (2), showing the temperature dependence as expected from the spin-boson model. (b) Rabi-like oscillations in sample no. 1 observed at the indicated temperatures using resonant microwaves of 16.5 GHz frequency. Solid lines are fits to exponentially decaying sine functions.

In order to preserve high contrast of the readout, we had to reduce the amplitude of the readout pulse at high temperatures, because escape from the excited qubit state to the deep well then becomes possible not only by quantum tunnelling but also by thermal activation over the barrier. Moreover, the width of the measured switching-current histogram of the readout dc SQUID increases, which reduces the contrast between the two qubit states. At high temperatures, we therefore separated the contributions of the two states to the readout SQUID switching-current distribution by a fitting procedure using weighted histograms of the two flux states.

Using the same experimental setup, we have also measured a sample of type no. 2 containing an $Al/AlO_x/Al$ phase qubit fabricated as described in Ref. [12]. This qubit features a smaller junction of about 1 μm^2 area which is shunted by a capacitor with SiN_x dielectric layer. It was demonstrated in Ref. [11] that replacing on-chip SiO_2 by SiN_x reduces the number of parasitic two-level fluctuators and significantly improves the coherence times of the qubit. As it is seen in Fig. 3, sample no. 2 showed Rabi oscillation decay times up to 100 ns—more than 1 order of magnitude longer than in Nb-SiO_2-based samples no. 1. These data measured in Erlangen are in good agreement with measurements at UC Santa Barbara which were performed using samples of the same batch [12].

The long coherence times of the qubit no. 2 indicate that in this sample, the energy levels are sufficiently narrow that we couple by microwaves only the lowest two levels and thus operate this qubit as a two-level system. Deeper potential wells in this case remain anharmonic enough not to result in poisoning of higher levels by microwaves applied at the frequency ω_{01}.

In Fig. 4, we plot the temperature dependence of the Rabi oscillation amplitude and decay time for sample no. 2. For each set of data points, we adjusted the magnetic field bias in order to match the energy level spacing $\Delta E \equiv \hbar\omega$ to be at resonance with the chosen microwave frequency, which is indicated in the legend. The microwave amplitude was adjusted to maximize the oscillation amplitude, resulting in Rabi oscillation frequencies of 135 and 205 MHz, respectively, for the two data sets at 7.4 and 8.0 GHz driving frequency. Remarkably, increasing the temperature up to about 300 mK, we observed nearly no effect on the oscillation amplitude and decay time. At yet higher temperatures, the oscillations rapidly decay and vanish completely at a temperature $T \approx T_\omega \equiv \hbar\omega/k_B$. The exact T_ω values are 0.355 K at $\omega = 2\pi \times 7.4$ GHz and 0.384 K at $\omega = 2\pi \times 8.0$ GHz.

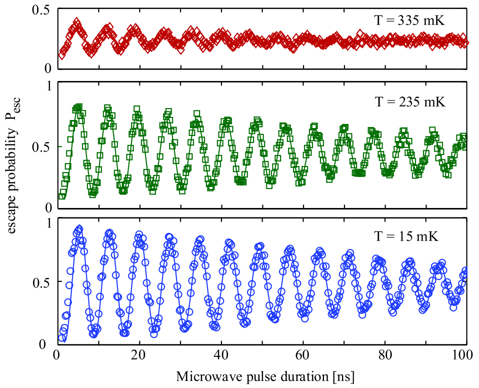

FIG. 3 (color online). Rabi oscillations observed in Al-based sample no. 2 featuring SiN_x insulation, at the indicated temperatures. The frequency of the driving microwave signal was 7.4 GHz. Solid lines are fits to exponentially decaying sine functions from which Rabi amplitude and decay time are extracted.

To measure the influence of temperature on the dephasing time T_2^* in sample no. 2, we performed a Ramsey-type experiment, in which two $\pi/2$-pulses separated by a variable duration are applied to the qubit. As expected, the frequency of the observed Ramsey fringes was equal to the detuning of the microwave from the resonance frequency. We took a set of data at 335 MHz detuning from the resonance at 8 GHz. Figure 5 shows the Ramsey oscillation amplitude and the extracted T_2^* time versus temperature. At temperatures up to about 180 mK, we measured a weak temperature dependence of the phase coherence time, which at $T = 15$ mK was $T_2^* \approx 90$ ns. At higher temperatures, the time T_2^* and fringe amplitude decrease and the oscillations vanish at about 380 mK.

Figure 5 also includes data from a direct measurement of the temperature dependence of the excited state decay time T_1. For better comparison, the data which was taken at an energy level spacing adjusted to 8.0 GHz has been multiplied by a factor of 1.49 in order to make it coincide at $T = 195$ mK with the data taken at 7.4 GHz. Below about 250 mK, both data sets show only weak temperature dependence. At higher temperatures, the T_1 times decrease rapidly and at an equal rate, both reaching zero at about 350 mK. The theoretical expectation for the T_1 time, for the spin-boson model, is [18]

$$T_1 = \frac{\hbar}{2\pi\Delta E}\frac{R}{R_Q}|A_{1,2}|^{-2}\left[1 + \coth\left(\frac{\Delta E}{2k_BT}\right)\right]^{-1}, \qquad (2)$$

where $R_Q = h/4e^2$ is the resistance quantum, R is the

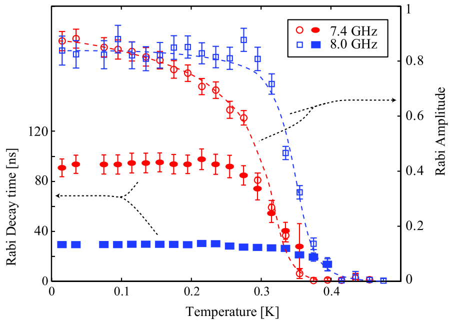

FIG. 4 (color online). Amplitude (right axis) and decay time (left axis) of Rabi oscillation observed in sample no. 2, plotted versus temperature. Dashed lines are guides to the eye.

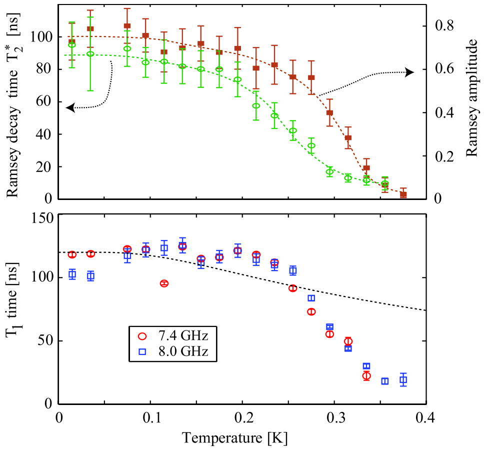

FIG. 5 (color online). Data obtained on sample no. 2. Top panel: Ramsey oscillation amplitude (filled squares, right axis) and decay time (open circles, left axis) vs temperature. Dashed lines are guides to the eye. Bottom panel: Directly measured decay time T_1 of the excited qubit state vs temperature. Two data sets correspond to different magnetic field biases, respectively, resulting in resonance at a frequency of 7.4 GHz (circles) and 8.0 GHz (squares). The 8.0 GHz data has been scaled as described in the text. The dashed line is a plot of Eq. (2), showing the theoretically expected temperature dependence for an energy level spacing of 8.0 GHz.

effective damping resistance, and $A_{1,2} = \langle 0 | \frac{\phi}{2\pi} | 1 \rangle$ is the interaction matrix element between the two states. The temperature dependence of the decay time is contained in the coth-term and is much less steep than the measured data shown in Fig. 5. Possibly, the temperature-independent decoherence in our data can be explained as being limited by microscopic two-level fluctuators at low temperatures. Increasing temperature, on one hand, may reduce the fluctuators-induced decoherence as some part of the two-level fluctuators gets saturated by energy absorbed from the thermal bath. On the other hand, high enough temperature leads to conventional decoherence of the qubit described by Eq. (2), which damps coherent oscillations at $T \approx T_\omega$. Detailed theoretical analysis of these competing decoherence mechanisms goes beyond the scope of our experimental work.

In conclusion, we presented measurements of the temperature dependence of coherent oscillations in two types of phase qubits. Rabi oscillations in the low-Q Josephson phase qubits fabricated using standard niobium processes with SiO_2 dielectric persisted at temperatures up to 0.9 K and above, with only a modest decrease in decay time. To observe the oscillations within their short coherence time, these qubits needed to be strongly driven and thus were operated in the multilevel (close to classical) limit. In contrast, high-Q aluminum-based phase qubits featuring SiN_x dielectric were operated in the two-level limit even at high temperatures. Coherence times measured in these quantum systems depend very weakly on temperature up to the point $T = T_\omega$, where the thermal energy $k_B T$ becomes equal to the energy level separation $\hbar\omega$. The abrupt decay of the coherence time at $T = T_\omega$ observed in high-Q qubits was not found in low-Q circuits. This qualitatively different temperature dependence in the above two types of samples allows us to distinguish between classical and quantum oscillations. Besides that, our results demonstrate that, without any significant degradation of their coherence times, the best available phase qubits can be operated in the quantum two-level regime at temperatures up to several 100 mK.

We acknowledge useful discussions with N. Grønbech-Jensen, N. Katz, J. E. Marchese, R. W. Simmonds, and F. Wilhelm. Partial financial support of this work by the Deutsche Forschungsgemeinschaft (DFG) and the European Office of Aerospace Research and Development (EOARD) is acknowledged.

---

*ustinov@physik.uni-erlangen.de

[1] Yu. Makhlin, G. Schön, and A. Shnirman, Nature (London) **398**, 305 (1999).
[2] M. H. Devoret, A. Wallraff, and J. M. Martinis, arXiv:cond-mat/0411174.
[3] D. Esteve and D. Vion, arXiv:cond-mat/0505676.
[4] G. Wendin and V. S. Shumeiko, arXiv:cond-mat/0508729.
[5] J. M. Martinis, S. Nam, J. Aumentado, and C. Urbina, Phys. Rev. Lett. **89**, 117901 (2002).
[6] J. Claudon, F. Balestro, F. W. J. Hekking, and O. Buisson, Phys. Rev. Lett. **93**, 187003 (2004).
[7] F. W. Strauch, S. K. Dutta, H. Paik, T. A. Palomaki, K. Mitra, B. K. Cooper, R. M. Lewis, J. R. Anderson, A. J. Dragt, C. J. Lobb, and F. C. Wellstood, arXiv:cond-mat/0703081.
[8] J. Lisenfeld, A. Lukashenko, and A. V. Ustinov (unpublished).
[9] R. W. Simmonds, K. M. Lang, D. A. Hite, D. P. Pappas, and J. M. Martinis, Phys. Rev. Lett. **93**, 077003 (2004).
[10] K. B. Cooper, M. Steffen, R. McDermott, R. W. Simmonds, S. Oh, D. A. Hite, D. P. Pappas, and J. M. Martinis, Phys. Rev. Lett. **93**, 180401 (2004).
[11] J. M. Martinis, K. B. Cooper, R. McDermott, M. Steffen, M. Ansmann, K. Osborn, K. Cicak, S. Oh, D. P. Pappas, R. W. Simmonds, and C. C. Yu, Phys. Rev. Lett. **95**, 210503 (2005).
[12] M. Steffen, M. Ansmann, R. McDermott, N. Katz, R. C. Bialczak, E. Lucero, M. Neeley, E. M. Weig, A. N. Cleland, and J. M. Martinis, Phys. Rev. Lett. **97**, 050502 (2006).
[13] M. Steffen, M. Ansmann, R. C. Bialczak, N. Katz, E. Lucero, R. McDermott, M. Neeley, E. M. Weig, A. N. Cleland, and J. M. Martinis, Science **313**, 1423 (2006).
[14] Hypres Inc., Elmsford, N.Y., USA.
[15] VTT Technical Research Center, Finland.
[16] N. Grønbech-Jensen and M. Cirillo, Phys. Rev. Lett. **95**, 067001 (2005).
[17] J. E. Marchese, M. Cirillo, and N. Grønbech-Jensen, Phys. Rev. B **73**, 174507 (2006).
[18] A. J. Legget, S. Chakravarty, and A. T. Dorsey *et al.*, Rev. Mod. Phys. **59**, 1 (1987).